Genotypic differences in systemic root responses to mechanical obstacles

Tino Colombi, Leah Eitelberg, Evelyne Kolb, Valérie Legué, Marie-Béatrice Bogeat-Triboulot

▶ **To cite this version:**

Tino Colombi, Leah Eitelberg, Evelyne Kolb, Valérie Legué, Marie-Béatrice Bogeat-Triboulot. Genotypic differences in systemic root responses to mechanical obstacles. Physiologia Plantarum, 2023, 175 (6), pp.e14094. 10.1111/ppl.14094 . hal-04533864

HAL Id: hal-04533864
https://hal.inrae.fr/hal-04533864

Submitted on 5 Apr 2024

HAL is a multi-disciplinary open access archive for the deposit and dissemination of scientific research documents, whether they are published or not. The documents may come from teaching and research institutions in France or abroad, or from public or private research centers.

L'archive ouverte pluridisciplinaire **HAL**, est destinée au dépôt et à la diffusion de documents scientifiques de niveau recherche, publiés ou non, émanant des établissements d'enseignement et de recherche français ou étrangers, des laboratoires publics ou privés.

Distributed under a Creative Commons Attribution - NonCommercial - NoDerivatives 4.0 International License

Check for updates

Received: 7 July 2023 | Accepted: 8 November 2023

DOI: 10.1111/ppl.14094

ORIGINAL RESEARCH

Physiologia Plantarum

Genotypic differences in systemic root responses to mechanical obstacles

Tino Colombi[1] | Leah Eitelberg[1] | Evelyne Kolb[2] | Valérie Legué[3] | Marie-Béatrice Bogeat-Triboulot[4]

[1]Department of Soil and Environment, Swedish University of Agricultural Sciences (SLU), Uppsala, Sweden

[2]PMMH, CNRS, ESPCI Paris, Université PSL, Sorbonne Université, Université Paris Cité, Paris, France

[3]Université Clermont Auvergne, INRAE, PIAF, Clermont-Ferrand, France

[4]Université de Lorraine, AgroParisTech, INRAE, UMR Silva, Nancy, France

Correspondence
Email: tino.colombi@slu.se

Present address
Leah Eitelberg, present address: Institute of Crop Science and Resource Conservation (INRES), University of Bonn, Bonn, Germany.

Funding information
Lantmännens Forskningsstiftelse, Grant/Award Number: 2019H005; Svenska Forskningsrådet Formas, Grant/Award Number: 2019-01189

Edited by G.P. Bienert

Abstract

As roots grow through the soil to forage for water and nutrients, they encounter mechanical obstacles such as patches of dense soil and stones that locally impede root growth. Here, we investigated hitherto poorly understood systemic responses of roots to localised root impedance. Seedlings of two wheat genotypes were grown in hydroponics and exposed to impenetrable obstacles constraining the vertical growth of the primary or a single seminal root. We deployed high-resolution *in vivo* imaging to quantify temporal dynamics of root elongation rate, helical root movement, and root growth direction. The two genotypes exhibited distinctly different patterns of systemic responses to localised root impedance, suggesting different strategies to cope with obstacles, namely stress avoidance and stress tolerance. Shallower growth of unconstrained seminal roots and more pronounced helical movement of unconstrained primary and seminal roots upon localised root impedance characterised the avoidance strategy shown by one genotype. Stress tolerance to localised root impedance, as exhibited by the other genotype, was indicated by relatively fast elongation of primary roots and steeper seminal root growth. These different strategies highlight that the effects of mechanical obstacles on spatiotemporal root growth patterns can differ within species, which may have major implications for resource acquisition and whole-plant growth.

KEYWORDS
in vivo imaging, mechanical obstacles, root circumnutation, root elongation, root growth direction, soil heterogeneity

1 | INTRODUCTION

The belowground environment of most terrestrial plants, including all arable crops, is shaped by the complex spatial arrangement of solids and pores in the soil, also referred to as soil structure (Rabot et al., 2018). Localised differences in soil porosity, pore size distribution, and pore connectivity result in spatial gradients of soil penetration resistance, water availability, and soil aeration capacity (Schlüter et al., 2019; Ebrahimi & Or, 2016; Hinsinger et al., 2009). Furthermore, soil structural heterogeneity leads to heterogeneous spatial distribution of organic carbon and plant-available nutrients (Keiluweit et al., 2017; Wang et al., 2020) and underpins the formation of spatially distinct microbial communities (Nunan et al., 2020; Borer et al., 2018; Ebrahimi & Or, 2016). The occurrence of these heterogeneities at the centimetre, millimetre, and sub-millimetre scale (Vogel et al., 2018) is a key feature distinguishing soil environments from aboveground

This is an open access article under the terms of the Creative Commons Attribution-NonCommercial-NoDerivs License, which permits use and distribution in any medium, provided the original work is properly cited, the use is non-commercial and no modifications or adaptations are made.
© 2023 The Authors. *Physiologia Plantarum* published by John Wiley & Sons Ltd on behalf of Scandinavian Plant Physiology Society.

environments of plants (Walter et al., 2009). Therefore, individual roots of the same plant can be exposed to distinctly different environmental conditions, and responses of root systems to soil heterogeneity are crucial to soil exploration by plants (Jin et al., 2013; York et al., 2016). Interactions between roots and heterogeneous edaphic conditions and the implications of these interactions for the access and acquisition of water and nutrients are essential to a holistic understanding of plant growth and crop productivity (Wang et al., 2020; Jin et al., 2017).

Root elongation rate and thus the access to water and nutrients in the soil are strongly influenced by the mechanical stress acting on the tip of a growing root (Colombi et al., 2018; Bengough et al., 2011; Liu et al., 2022a). As roots grow into deeper and thus denser soil layers, root mechanical stress gradually increases, decreasing root elongation rate (Lynch & Wojciechowski, 2015; Kautz et al., 2013; Bengough et al., 2011). In addition to gradual changes, the mechanical stress acting on a root tip can increase suddenly. Such sudden increases in root mechanical stress typically occur when roots encounter a hardpan or impenetrable objects such as stones (Kolb et al., 2017; Martínez et al., 2016) or when roots leave macropores and re-enter the soil matrix (Jin et al., 2013). A sudden increase of root mechanical stress also reduces root elongation rate (Sjulgård et al., 2021; Croser et al., 1999; Quiros et al., 2022) and can furthermore lead to a deflection of the root tip, thereby changing the growth direction of roots (Roué et al., 2020; Atkinson et al., 2020; Dexter, 1986). Greater root mechanical stress also increases the nutation amplitude of the helical movement of roots (Martins et al., 2020) and root circumnutation has been linked to the avoidance of obstacles and plant establishment on rocky soil (Taylor et al., 2021). Hence, sudden changes in root mechanical stress directly affect root growth rate and direction, ultimately affecting the soil volume and layers in which plants forage for water and nutrients.

Sudden increases in root mechanical stress due to penetrable and impenetrable mechanical obstacles typically affect only a part of the root system. Thus, mechanical obstacles in the soil, such as hardpans, stones, and pore walls, impede root growth locally. Effects of root mechanical stress on elongation rate, root growth direction, and helical movement of impeded roots are well documented (Sjulgård et al., 2021; Croser et al., 1999; Quiros et al., 2022; Roué et al., 2020; Atkinson et al., 2020; Dexter, 1986; Martins et al., 2020). Localised impedance of one or several axial roots can also affect the remaining unconstrained roots of the same root system, but such systemic responses to mechanical obstacles in soil are poorly understood. Plants have been shown to reduce root growth in rocky substrate if the root system has access to more favourable soil conditions (Semchenko et al., 2008). Similarly, compensatory root growth into loose soil upon localised soil compaction has been demonstrated (Bingham & Bengough, 2003; Pfeifer et al., 2014). However, it remains unclear if plants slowly increase root proliferation into patches with favourable conditions or if mechanical obstacles have immediate systemic effects on root growth rate and trajectory. To better understand how plants cope with mechanical obstacles and how this affects soil exploration, we need to explicitly address systemic responses of root systems to localised root impedance.

In vivo imaging of spatial and temporal root growth patterns can provide novel insights into plant-environment interactions (Walter et al., 2015; Ruts et al., 2012; Atkinson et al., 2020) and offers possibilities to elucidate root responses to changing environmental conditions at high spatiotemporal resolution (Quiros et al., 2022; Bizet et al., 2015; Roué et al., 2020; Basu et al., 2007; Ruts et al., 2013). Achievable throughput, image resolution, and measurement frequency of approaches allowing for visualisation of roots in soil, such as X-ray or neutron imaging, are limited (Tötzke et al., 2017; Tracy et al., 2012; Zarebanadkouki et al., 2013). Experimental systems using transparent growth media, including hydroponics, can overcome these limitations and are therefore, suitable to investigate root-soil interactions at high spatiotemporal resolution. Gel-based systems (Roué et al., 2020) and hydroponics (Bizet et al., 2016) were used to reveal temporal patterns of root tip deflection and bending of roots encountering mechanical obstacles. Similarly, *in vivo* quantification of helical root movement (Martins et al., 2020) and responses of root elongation to suddenly occurring osmotic stress (Bizet et al., 2015) have been achieved in transparent growth media. Mechanical obstacles occurring in soil, such as dense soil patches, stones, and pore walls, affect numerous soil properties and processes (Ebrahimi & Or, 2016; Naseri et al., 2019; Banfield et al., 2017), while obstacles placed into hydroponics allow to specifically target effects of root impedance. Thus, hydroponics allows the disentangling of the effects of mechanical stress from other soil properties associated with mechanical obstacles.

The aim of the current study was to assess systemic effects of mechanical obstacles on spatial and temporal growth patterns of roots in wheat (*Triticum aestivum* L.). To do so, we grew wheat seedlings in hydroponics and exposed roots to mechanical obstacles that constrained the vertical growth of either the primary or a single seminal root. *In vivo* time-lapse imaging at high spatiotemporal resolution was deployed in conjunction with particle image velocimetry to quantify systemic responses of root elongation rate, helical root movement, and root growth direction to localised root impedance. We performed experiments with two different wheat varieties to elucidate whether strategies to cope with mechanical obstacles differ between genotypes of the same species.

2 | MATERIALS AND METHODS

2.1 | Plant material

We used two different wheat varieties, 'Happy' and 'Maggie' that respond differently to increasing soil density. As shown in an earlier study, the adverse impact of increasing soil density on the elongation rate of embryonic roots (i.e. primary and seminal roots) is significantly more pronounced in Happy than in Maggie (Colombi et al., 2019). The average seed weight of both varieties was determined from 200 seeds (Maggie: 48 mg seed^{-1}; Happy: 40 mg seed^{-1}), and seeds with uniform weight (average seed weight ± 10%) were selected for the experiments.

2.2 | Experimental set-up and treatments

Experiments were conducted in hydroponics using half-strength Hoagland nutrient solution (Hoagland's No. 2 Basal Salt Mixture; Sigma Aldrich) adjusted to pH 5.8 with NaOH solution (Bizet

13993054, 2023, 6, Downloaded from https://onlinelibrary.wiley.com/doi/10.1111/ppl.14094 by Inrae - Dipso, Wiley Online Library on [04/04/2024]. See the Terms and Conditions (https://onlinelibrary.wiley.com/terms-and-conditions) on Wiley Online Library for rules of use; OA articles are governed by the applicable Creative Commons License

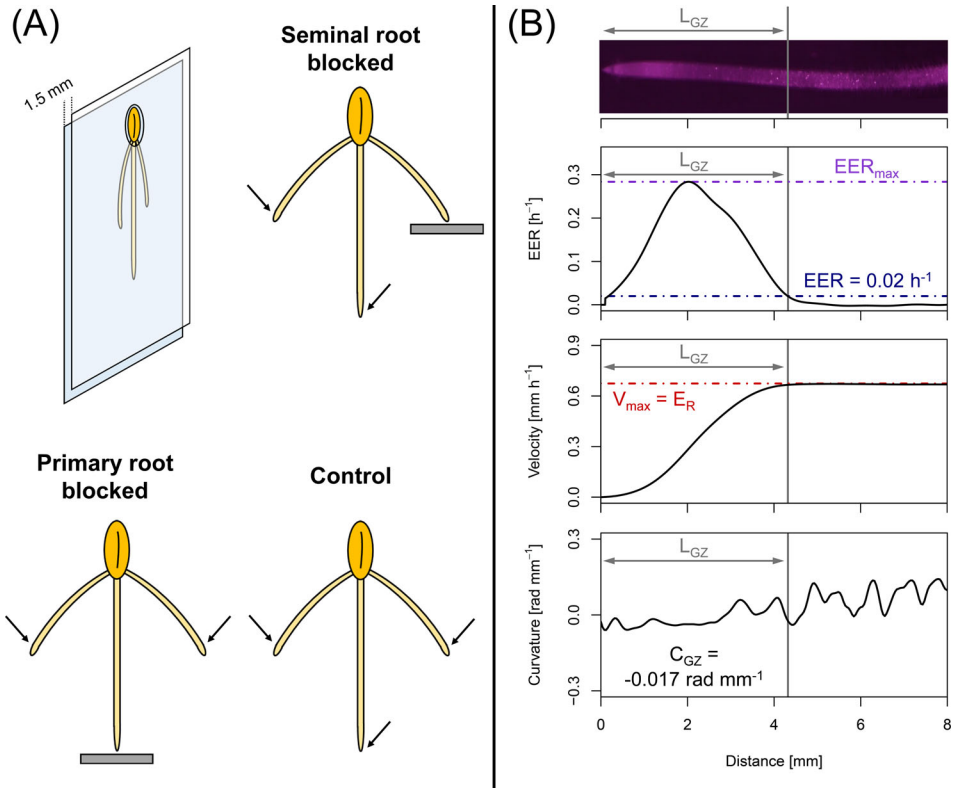

FIGURE 1 (A) Schematic representation of growth cells made of two vertical Plexiglas plates placed into a hydroponics system and the different treatments included in the current study with black arrows indicating unconstrained roots for which growth parameters were quantified. (B) Illustration of root growth parameters derived from image analysis with KymoRod (Bastien et al., 2016), namely: elemental elongation rate (EER [h^{-1}]) as a proxy for cell elongation rate; length of the root growth zone (L_{GZ} [mm]) defined as the distance between root tip and the position along the root where EER = 0.02 [h^{-1}]; root elongation rate (E_R [mm h^{-1}]) corresponding to the velocity at the end of the growth zone (V_{max} [mm h^{-1}]); and the average curvature of the root growth zone (C_{GZ} [rad mm^{-1}]) obtained from the curvature profile along the root growth zone.

et al., 2015). The hydroponics system consisted of two containers, a reservoir container with 10 L volume and a growth container with 1.8 L volume (height/width/depth: 24/15/5 cm) made from transparent Plexiglas. Three air pumps (Pro Silent a100, JBL GmbH & Co. KG) were used to aerate the nutrient solution in the reservoir container. For the experiments, 6 L of aerated nutrient solution was circulated between the reservoir container and growth container with an aquarium pump (Newa Jet 400, Newa Tecno Industrial SRL) at a rate of 54 L h^{-1}. The nutrient solution was renewed once per week.

Seedlings were grown in growth cells made of two 2 mm thick Plexiglas plates that were placed vertically into the growth container of the hydroponics system. The two Plexiglas plates were arranged parallel with a 1.5 mm gap. This allowed roots to grow freely between the plates without mechanical resistance while staying in the image plane. To fix the seed in place, a hole of 7 mm diameter was cut out from the front plate, and filter paper was used to hold the seed. Horizontal impenetrable obstacles in the form of microscope slides covered with sand (0.5–1.0 mm grain size) could be added to the growth cells. The obstacles constrained either the primary root or one seminal root from growing further down. In addition to these two treatments in which plants were exposed to mechanical obstacles, a control treatment without mechanical obstacles was included in the study (Figure 1A). Every variety-treatment combination was replicated four times (n = 4).

2.3 | Growth conditions and image acquisition

Experiments were conducted in a dark and temperature-controlled room at a constant temperature of 21.8°C. Seeds were pre-germinated in an upright position on filter paper soaked in half-strength Hoagland solution (pH adjusted to 5.8 with NaOH solution) for 56 h. Seedlings with approximately 12 mm long primary roots and approximately 7 mm long seminal roots were selected for the experiments. A single seedling was transplanted into a growth cell, and the growth cell was put into the growth container of the hydroponics system with the seed halfway immersed into the nutrient solution.

Root growth was recorded for 24 h in 2-min intervals using a 24-megapixel camera (Canon EOS 750d, Canon) equipped with a macro lens (EF-S 35 mm f/2.8 Macro IS STM, Canon). The infrared filter of the camera was removed, and illumination was provided by two rows of 20 infrared LEDs with 830 nm wavelength (TSHG8400 Vishay, 830 Nm IR LED, Vishay Intertechnology, Inc.). The LEDs were mounted above and below the growing seedling to illuminate the roots at an angle of 10°. Due to the illumination with infrared LEDs at such a flat angle, textures at the root surface appeared as patterns of bright points (Figure 1B; Bizet et al., 2015; Quiros et al., 2022). The distance between the camera lens and the roots was 75 mm, resulting in a pixel edge length of 8.55 µm.

2.4 | Image processing and analysis

In all treatments, an image series of 180 consecutive images covering a growth period of 6 h were analysed. For the two treatments in which roots were exposed to mechanical obstacles, we included images taken during 2 h immediately before the obstacle was reached and images taken during 4 h immediately after the obstacle was reached. Primary and seminal root lengths at the start of the image series from treatments with mechanical obstacles were determined

13993054, 2023, 6, Downloaded from https://onlinelibrary.wiley.com/doi/10.1111/ppl.14094 by Inrae - Dipso, Wiley Online Library on [04/04/2024]. See the Terms and Conditions (https://onlinelibrary.wiley.com/terms-and-conditions) on Wiley Online Library for rules of use; OA articles are governed by the applicable Creative Commons License

manually in ImageJ (version 1.53e; National Institute of Health). These measurements were used to select the start of the image series from treatments without mechanical obstacles to ensure similar root lengths across treatments and genotypes (Figure S1). Images were cropped in ImageJ to obtain image series of individual axial roots.

Image series of all roots that did not encounter a mechanical obstacle, i.e. unconstrained primary and seminal roots (Figure 1A), were analysed with the software KymoRod (Bastien et al., 2016) in a Matlab 2019b environment (The Mathworks). The segmentation threshold, filter size, and contour smoothing were set manually for every image series, while the remaining image analysis parameters were fixed for all image series (Table S1). In KymoRod, particle image velocimetry is performed using patterns of bright points on the root surface (Figure 1B). This procedure yields displacement fields and, thus velocity profiles as a function of the curvilinear abscissa along the root skeleton. The spatial derivation of the velocity profiles corresponds to the relative elemental elongation rate (EER [h^{-1}]) along the root skeleton (Bastien et al., 2016). We set the length of the growth zone (L_{GZ} [mm]) between the root tip and the position on the curvilinear abscissa along the root skeleton where EER dropped below 0.02 h^{-1}. The maximum relative elemental elongation rate (EER_{max} [h^{-1}]) within the root growth zone was used as a proxy for the relative cell elongation rate (Youssef et al., 2018). The root elongation rate (E_R [mm h^{-1}] was set as the velocity at the end of the root growth zone (Figure 1B). For statistical analyses, we used hourly mean values of L_{GZ}, EER_{max}, and E_R.

Root curvature data provided by KymoRod (Bastien et al., 2016) was used to characterize temporal patterns of helical movement of primary and seminal roots and the growth direction of seminal roots. Since active responses of roots to environmental stimuli occur in the root growth zone, we obtained the average curvature of the entire root growth zone (C_{GZ} [rad mm^{-1}]) from root curvature profiles and information on L_{GZ} (Figure 1B). The average curvature along the root growth zone, hereafter referred to as the curvature of the root growth zone, was then used to quantify helical root movement and root growth direction. The difference between maximum and minimum curvature of the growth zone occurring within one hour of root growth served as a proxy for the nutation amplitude of helical movement of unconstrained primary and seminal roots. To ensure that the difference between maximum and minimum curvature within one hour adequately captured the amplitude of helical root movement across treatments and genotypes, we additionally calculated the nutation amplitude over two hours. Effects of localised root impedance on the growth direction of unconstrained seminal roots were quantified using hourly mean values of the curvature of the root growth zone. The sign of curvature values of seminal roots located on the left side of the seed was changed (i.e. multiplied by −1) so that curvature towards the vertical was denoted in both seminal roots by a negative curvature value. Temporal changes in root curvature (ΔC_t [rad mm^{-1}]) were then calculated as:

$$\Delta C_t = C_t - \frac{C_{(-2)} + C_{(-1)}}{2} \quad (1)$$

In seedlings exposed to obstacles, C_t denotes the average curvature of the root growth zone during the t^{th} hour (t = 1, 2, 3, 4) after encountering the obstacle. The average curvature of the root growth zone during the first and second hour before encountering the obstacle is indicated by $C_{(-2)}$ and $C_{(-1)}$, respectively. In seedlings grown without mechanical obstacles, $C_{(-2)}$ and $C_{(-1)}$ denote the curvature during the first two hours of the image series, and C_t denotes the curvature during the third, fourth, fifth, and sixth hours of the image series. ΔC_t <0 indicated a change in the growth direction of seminal roots towards more vertical growth, while ΔC_t >0 indicated a change in the growth direction towards more horizontal growth. Seminal root angles at the beginning of each image series were assessed manually in ImageJ using the angle between the vertical and the root 5 mm from the root base.

2.5 | Statistics

All statistical analyses were done in R version 4.0.2 using the packages 'stats' and 'nlme' (R Core Team, 2020; Pinheiro et al., 2013) and primary and seminal roots were evaluated separately. Effects of time,

TABLE 1 Summary statistics on the effects of time (T), treatment (Trt), genotype (GT), and their interactions on hourly mean root elongation rate (E_R) and the nutation amplitude of helical root movement of unconstrained roots. The amplitude of helical root movement was quantified as the difference between the maximum ($Curv_{max}$) and minimum ($Curv_{min}$) curvature of the root growth zone within each hour of measurements. *P*-values were derived from linear-mixed models that included the sample effect as a random factor to account for repeated measurements (n = 4). The nutation amplitude of helical root movement was log-transformed

Trait	E_R [mm h^{-1}]		ln($Curv_{max}$-$Curv_{min}$) [rad mm^{-1}]	
Root class	Primary root	Seminal root	Primary root	Seminal root
p(T)	< 0.001	< 0.001	< 0.05	0.18
p(Trt)	0.23	0.72	0.08	0.21
p(GT)	0.78	0.76	0.45	0.77
p(T:Trt)	0.31	0.16	0.99	0.33
p(T:GT)	< 0.05	0.90	< 0.01	0.10
p(Trt:GT)	0.89	0.92	0.60	0.39
p(T:Trt:GT)	0.16	0.45	< 0.001	< 0.01

13993054, 2023, 6, Downloaded from https://onlinelibrary.wiley.com/doi/10.1111/ppl.14094 by Inrae - Dipso, Wiley Online Library on [04/04/2024]. See the Terms and Conditions (https://onlinelibrary.wiley.com/terms-and-conditions) on Wiley Online Library for rules of use; OA articles are governed by the applicable Creative Commons License

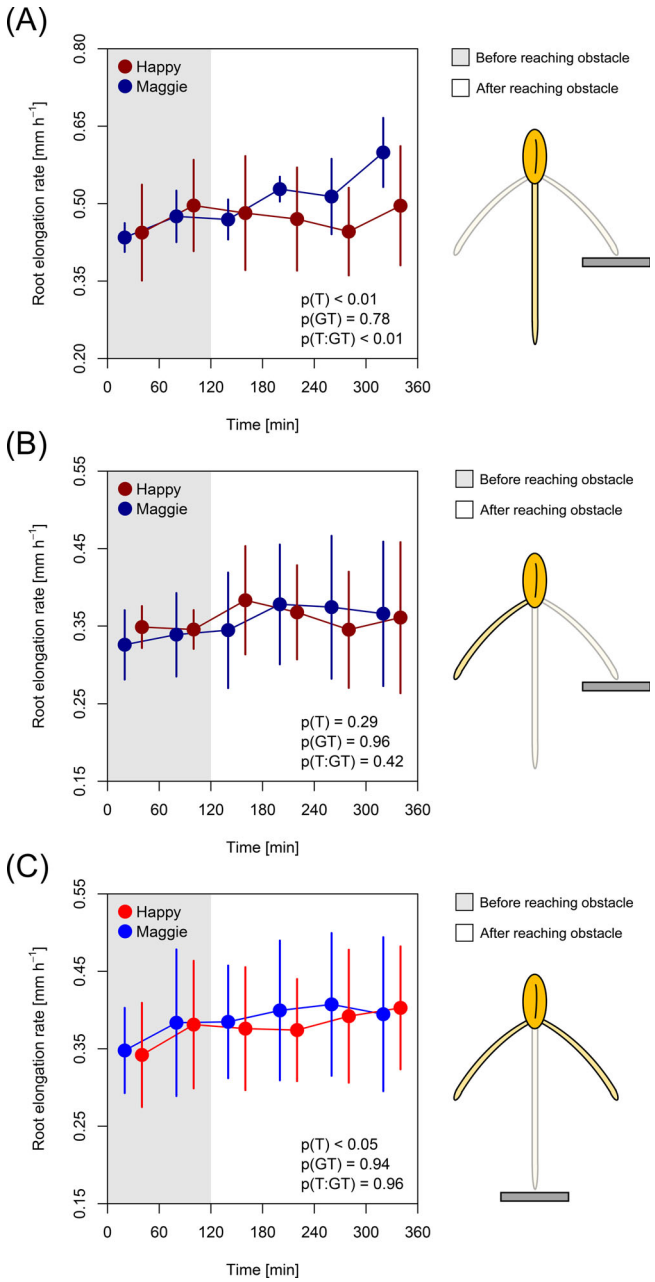

FIGURE 2 Effects of localised root impedance on root elongation rate of unconstrained (A) primary and (B) and (C) seminal roots. Grey shaded area indicates period before the obstacle was reached. Area without shading indicates period after the obstacle was reached and vertical growth of (A) and (B) one seminal root and (C) the primary root was constrained. Error bars denote standard error and *p*-values were derived from linear-mixed models that included the sample effect as a random factor to account for repeated measurements (n = 4).

treatment, genotype, and their interactions on root growth parameters were evaluated with linear mixed models that included the sample effect as a random factor to account for repeated measurements. Genotype and treatment were treated as fixed categorical variables, and time was treated as a fixed continuous variable. The nutation amplitude of helical root movement described by the difference between maximum and minimum curvature of the growth zone within one hour of root growth was log-transformed to ensure normal distribution of residuals. Analysis of covariance was used to test for the significance of the effects of time, treatment, genotype, and their interactions on the different root growth parameters. Linear regressions were used to explain root elongation rate as a function of the length of the growth zone and maximum elemental elongation rate.

3 | RESULTS

3.1 | Effects of localised root impedance on elongation rate of unconstrained roots

Significant effects of time on the elongation rate of unconstrained primary and seminal roots occurred ($p < 0.001$; Table 1), reflecting the general trend of increased root elongation rate over the analysed growth period of six hours (Figure 2, Supplemental Figure S2). For primary as well as seminal roots, the maximum elemental elongation rate yielded stronger correlations with root elongation rate ($R^2 > 0.83$) than the length of the growth zone ($R^2 < 0.35$; Supplemental Figure S3) across treatments, genotypes, and time points. Hence, differences in maximum elemental elongation rate and, thus the cell elongation rate was a stronger predictor for differences in root elongation rate than differences in the length of the root growth zone.

We found significant time-genotype interaction effects on the elongation rate of primary roots ($p < 0.05$; Table 1). Evaluating different treatments separately showed that these time-genotype interaction effects were significant only if vertical growth of one seminal root was constrained ($p < 0.01$; Figure 2A) and not if all roots could grow freely without encountering obstacles ($p = 0.49$; Figure S2A). Before reaching the obstacle, Happy and Maggie showed almost identical primary root elongation rates. Over the four hours after the vertical growth of one seminal root was constrained, i.e. after one seminal root reached the obstacle, the root elongation rate of primary roots in Maggie increased by more than 25% (Figure 3). This increase was comparable to the temporal increase in primary root elongation rate occurring over the same time in Maggie seedlings not exposed to obstacles (Figure S2A). In Happy, however, the primary root elongation rate remained almost constant during the four hours following the impedance of one seminal root (Figure 3), while it increased by 28% in seedlings that were not exposed to obstacles (Figure S2A). Such time-genotype interaction effects did not occur for the elongation rate of seminal roots ($p = 0.90$; Table 1). Temporal patterns of seminal root elongation rate did not differ significantly between genotypes if vertical growth of one seminal ($p = 0.42$; Figure 2B) or the primary root was constrained ($p = 0.96$; Figure 2C), or if no root was exposed to an obstacle ($p = 0.33$; Figure S2B).

3.2 | Helical root movement in response to localised root impedance

Different response patterns between genotypes also occurred for the difference between maximum and minimum curvature of the root

13993054, 2023, 6, Downloaded from https://onlinelibrary.wiley.com/doi/10.1111/ppl.14094 by Inrae - Dipso, Wiley Online Library on [04/04/2024]. See the Terms and Conditions (https://onlinelibrary.wiley.com/terms-and-conditions) on Wiley Online Library for rules of use; OA articles are governed by the applicable Creative Commons License

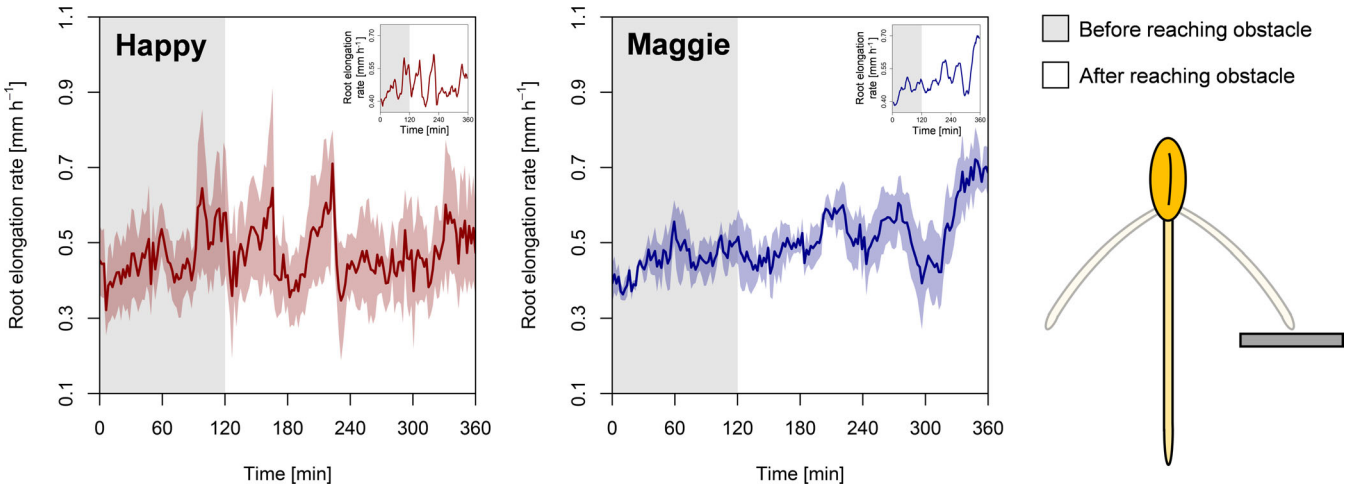

FIGURE 3 Elongation rate of unconstrained primary roots during 6 h measurement period. Grey shaded area indicates period before the obstacle was reached and area without shading indicates period after the obstacle was reached and vertical growth of one seminal root was constrained. Red and blue curves and shading represent mean values and standard error, respectively (n = 4). Insets depict smoothened root elongation rate using a 10-min moving average.

growth zone during one hour of root growth, representing the nutation amplitude of helical root movement. We found significant time-genotype interaction effects ($p < 0.01$) and time-treatment-genotype interaction effects ($p < 0.001$) on the nutation amplitude of helical movement of unconstrained primary roots (Table 1). As for root elongation rate, the most pronounced genotypic differences occurred in primary roots of seedlings in which vertical growth of one seminal root was constrained, as indicated by highly significant time-genotype interaction effects ($p < 0.001$; Figure 4A). Before the seminal root reached the obstacle, the amplitude of the helical movement of primary roots was comparable between Happy and Maggie. During the four hours following the impedance of one seminal root, the amplitude of helical movement of primary roots in Happy more than doubled. The amplitude of the helical movement of primary roots in Maggie, however, decreased by approximately 40% after one seminal root was constrained from growing further down (Figure 5). If no root was impeded, similar temporal patterns of the nutation amplitude of helical movement of primary roots occurred in Maggie and Happy, and no significant time-genotype interaction effects were found ($p = 0.58$; Figure S4A). Similar results on time-genotype interaction effects on the nutation amplitude of root helical movement occurred when the nutation amplitude was calculated over two hours (Supplemental Table S2). We, therefore, suggest that calculating the nutation amplitude using the minimum and maximum curvature within one hour of measurement was adequate to quantify the intensity of the helical movement of primary roots.

The amplitude of helical movement of seminal roots also showed significant time-treatment-genotype interaction effects ($p < 0.01$; Table 1). As observed in primary roots, temporal patterns of the amplitude of helical movement of seminal roots differed significantly between Happy and Maggie if one seminal root was impeded ($p < 0.01$). In Happy, the amplitude of helical movement of unconstrained seminal roots increased by 45% over four hours of constrained vertical growth of the other seminal root. In contrast, the amplitude of the helical movement of the unconstrained seminal roots of Maggie decreased by around 20% if the other seminal root was constrained from growing further down (Figure 4B). No significant interaction effects between time and genotype on the helical movement of seminal roots were observed if vertical growth of the primary root was constrained ($p = 0.70$; Figure 4C) or if no root was exposed to a mechanical obstacle ($p = 0.37$; Figure S4B). Hence, temporal patterns of the helical movement of seminal roots did not differ significantly between Happy and Maggie if the primary root was impeded or if no roots were constrained from growing down. As for primary roots, very similar results occurred when the nutation amplitude of seminal roots was calculated over two hours of growth (Table S2), indicating that one-hour intervals adequately captured the intensity of root helical movement.

3.3 | Changing growth direction of seminal roots upon localised root impedance

Root angle measurements before roots reached the obstacle showed that Happy had significantly shallower seminal roots than Maggie ($p < 0.01$; Figure 6A). Temporal patterns of growth direction of unconstrained seminal roots quantified as the difference in the curvature of the root growth zone before and after the obstacle was reached (Equation 1), differed between genotypes. Significant time-genotype ($p < 0.01$), treatment-genotype ($p < 0.05$), and time-treatment-genotype ($p < 0.01$) interaction effects occurred for the difference in curvature of the root growth zone (Table 2). Comparing changes in the curvature of the growth zone between treatments revealed that the two genotypes exhibited distinctly different temporal patterns of growth direction of unconstrained seminal in response to localised root impedance. In Happy, seminal roots of seedlings not exposed to mechanical obstacles became steeper over time. Such changes in growth direction towards the vertical of unconstrained

13993054, 2023, 6, Downloaded from https://onlinelibrary.wiley.com/doi/10.1111/ppl.14094 by Inrae - Dipso, Wiley Online Library on [04/04/2024]. See the Terms and Conditions (https://onlinelibrary.wiley.com/terms-and-conditions) on Wiley Online Library for rules of use; OA articles are governed by the applicable Creative Commons License

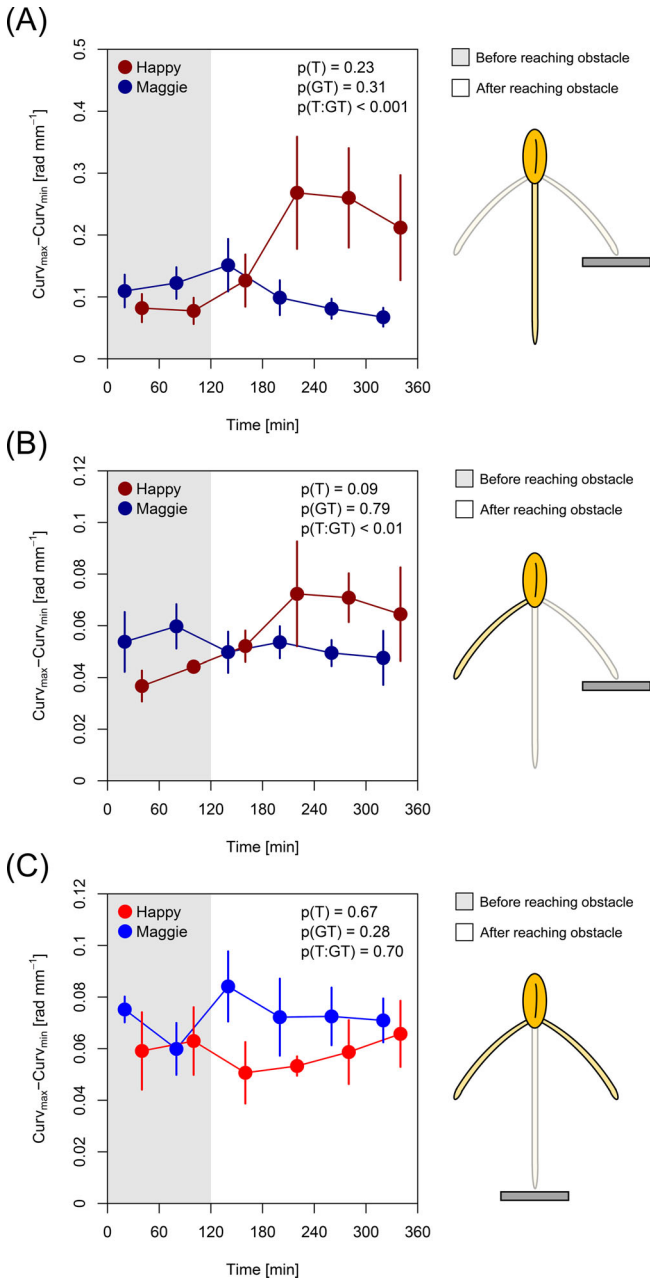

FIGURE 4 Effects of localised root impedance on nutation amplitude of helical root movement of unconstrained (A) primary and (B) and (C) seminal roots. The nutation amplitude was assessed as the difference between maximum ($Curv_{max}$) and minimum curvature ($Curv_{min}$) of the root growth zone within one hour of root growth. Grey shaded area indicates period before the obstacle was reached. Area without shading indicates period after the obstacle was reached and vertical growth of (A) and (B) one seminal root and (C) the primary root was constrained. Error bars denote standard error and *p*-values were derived from linear-mixed models that included the sample effect as a random factor to account for repeated measurements (n = 4).

seminal roots were less pronounced if the vertical growth of the other seminal root was constrained (Figure 6B). If the primary root of Happy was constrained from growing further down, seminal roots became shallower (Figure 6C). Changes in the growth direction of seminal roots towards the vertical over time did not occur in seedlings of Maggie that were grown without mechanical obstacles. The seminal roots of Maggie became steeper when the vertical growth of primary roots was constrained (Figure 6C). Similar yet non-significant changes in the growth direction of unconstrained seminal roots occurred if the other seminal root was impeded (Figure 6B).

Thus, the seminal roots of Happy, which grew relatively shallow at the start of the image series, became even shallower in response to localised root impedance compared to seedlings grown without mechanical obstacles. In contrast, seminal roots of Maggie grew already relatively steep from the start and localised root impedance, especially the impedance of the primary root, led to even steeper root growth direction (Figure 6A-C).

4 | DISCUSSION

Localised root impedance and, thus a sudden increase of root mechanical stress typically occurs if roots enter a dense soil matrix or encounter impenetrable objects such as stones (Jin et al., 2013; Kolb et al., 2017). In natural soil environments, increasing localised root impedance often coincides with further changes in soil conditions. Gas transport capacity typically decreases with higher soil density, resulting in changes in the soil atmosphere, shifts in the composition of localised microbial communities, and alterations of biochemical processes (Ebrahimi & Or, 2016; Keiluweit et al., 2017; Borer et al., 2018). Similarly, hydraulic properties at soil-stone interfaces differ from conditions in the soil matrix (Naseri et al., 2019). Given these interactions among different soil properties, disentangling the effects of localised root impedance from the effects of other soil physical, chemical, and biological properties on roots is challenging (Vogel et al., 2018; Wang et al., 2020). To specifically quantify the effects of localised root impedance, we placed impenetrable obstacles into a hydroponics system that constrained the vertical growth of either the primary root or one seminal root of wheat seedlings (Figure 1A). Hydroponics further allowed for *in vivo* quantification of root elongation rate at high spatiotemporal resolution. As in previous studies, we deployed particle image velocimetry to obtain the length of the root growth zone (Figure 1B; Basu et al., 2007; Bizet et al., 2015, 2016; Bastien et al., 2016; Youssef et al., 2018), which we then used to quantify helical movement and growth direction of unconstrained roots.

The general trend of increasing root elongation rate over time observed here (Figure 2; Figure S2) corresponds to previous studies that reported temporal increases in the elongation rate of newly emerged axial (Croser et al., 1999; Youssef et al., 2018) and lateral roots (in 't Zandt et al., 2015). Performing experiments with two different wheat genotypes enabled us to demonstrate that responses to mechanical obstacles can differ within a single species. No genotypic differences in the dynamics of the seminal root elongation rate occurred, but the temporal patterns of the primary root elongation rate differed significantly between the two genotypes (Table 1). The primary root elongation rate of Maggie increased over time if one

13993054, 2023, 6, Downloaded from https://onlinelibrary.wiley.com/doi/10.1111/ppl.14094 by Inrae - Dipso, Wiley Online Library on [04/04/2024]. See the Terms and Conditions (https://onlinelibrary.wiley.com/terms-and-conditions) on Wiley Online Library for rules of use; OA articles are governed by the applicable Creative Commons License

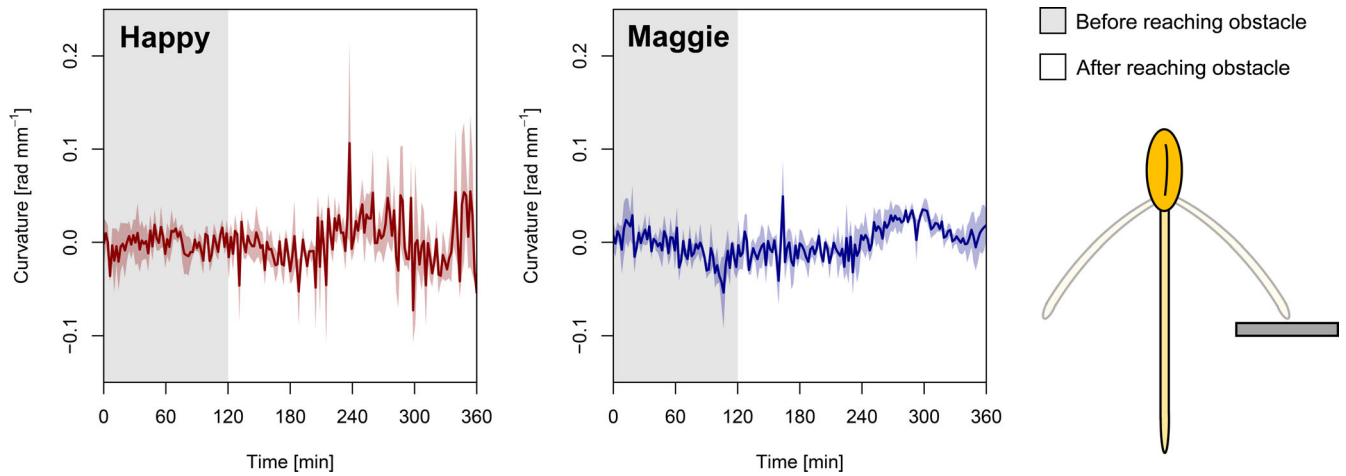

FIGURE 5 Curvature of the growth zone of unconstrained primary roots during 6 h measurement period. Grey shaded area indicates period before the obstacle was reached and area without shading indicates period after the obstacle was reached and vertical growth of one seminal root was constrained. Red and blue curves and shading represent mean values and standard error, respectively (n = 4).

seminal root was impeded (Figure 2A). The same pattern occurred in Maggie and Happy seedlings not exposed to mechanical obstacles (Figure S2A). In Happy, however, the primary root elongation rate did not increase and remained nearly constant after the vertical growth of one seminal root was constrained, suggesting a systemic response to localised root impedance (Figure 2A). Increased root proliferation in loose soil patches upon localised soil compaction (Bingham & Bengough, 2003; Pfeifer et al., 2014) and avoidance of rocky substrate (Semchenko et al., 2008) have been demonstrated in plants that were several days or weeks old. We showed here that the root elongation rate of unconstrained roots may change within hours in response to localised root impedance, indicating a near-immediate systemic response to mechanical obstacles.

Helical root movement and, thus root circumnutation has been linked to thigmotropism, i.e. the ability to respond to touch stimuli (Loshchilov et al., 2021; Migliaccio et al., 2013), facilitating root growth around obstacles and plant establishment in rocky soil (Taylor et al., 2021). It has been shown that the nutation amplitude of helical root movement increases if the mechanical stress acting on the tip of the same root increases (Martins et al., 2020). Here, we found systemic responses of helical root movement to mechanical obstacles and show that these responses can differ between genotypes of the same species (Table 1). Within two hours following the impedance of one seminal root, the nutation amplitude of helical movement of unconstrained primary and seminal roots in Happy increased by 100% and 45%, respectively. In contrast, the amplitude of helical root movement in Maggie remained constant or decreased in response to localised root impedance (Figure 4). Effects of mechanical obstacles on temporal patterns of the growth direction of unconstrained seminal roots also differed between the two genotypes (Table 2). The seminal roots of Happy, which had shallower seminal roots than Maggie (Figure 6A), became steeper over time if no mechanical obstacles were included. If the vertical growth of primary roots was constrained, seminal roots in Happy became shallower. In contrast, the unconstrained seminal roots of Maggie became steeper if primary root growth was constrained (Figure 6C). Similar yet less pronounced growth direction patterns of unconstrained seminal roots occurred if one seminal root was impeded (Figure 6B). Changes in root growth direction upon sudden changes of the mechanical stress at the root tip have been reported previously (Roué et al., 2020; Atkinson et al., 2020; Dexter, 1986) and we show here that such responses can also be systemic.

The two wheat genotypes included in the current study exhibited distinctly different responses to mechanical obstacles (Tables 1 and 2). Genotype-specific responses to other edaphic stresses, including drought (Li et al., 2021; Katuwal et al., 2020; Songsri et al., 2008) and flooding (Pedersen et al., 2021; Bailey-Serres et al., 2012; Thomson et al., 1992) have been reported previously and stress response have been categorized as 'stress avoidance' or 'stress tolerance'. Avoidance refers to responses enabling plants to circumvent a stress, such as increased rooting depth upon drought (Songsri et al., 2008) and shallower rooting in response to flooding (Bailey-Serres et al., 2012). Tolerance on the other hand, describes responses enabling plants to withstand stress, such as the formation of root cortical aerenchyma in flooded soil (Pedersen et al., 2021; Thomson et al., 1992). Our study suggests that responses to mechanical obstacles can also be classified into these two categories. Shallower seminal roots (Figure 6) and reduced primary root elongation rate (Figure 2; Figure S2) upon localised root impedance, as shown by Happy, suggest avoidance of further obstacles that could compromise vertical root growth. Given the association between helical root movement and the ability to avoid mechanical obstacles (Taylor et al., 2021), more pronounced helical root movement upon localised root impedance, as observed in Happy (Figure 4), likely facilitates the avoidance of potential future obstacles. In contrast, steeper seminal root growth (Figure 6) and relatively fast elongation of primary roots (Figure 2) upon localised root impedance, as shown by Maggie, contribute to deeper root growth, which indicates stress tolerance.

13993054, 2023, 6, Downloaded from https://onlinelibrary.wiley.com/doi/10.1111/ppl.14094 by Inrae - Dipso, Wiley Online Library on [04/04/2024]. See the Terms and Conditions (https://onlinelibrary.wiley.com/terms-and-conditions) on Wiley Online Library for rules of use; OA articles are governed by the applicable Creative Commons License

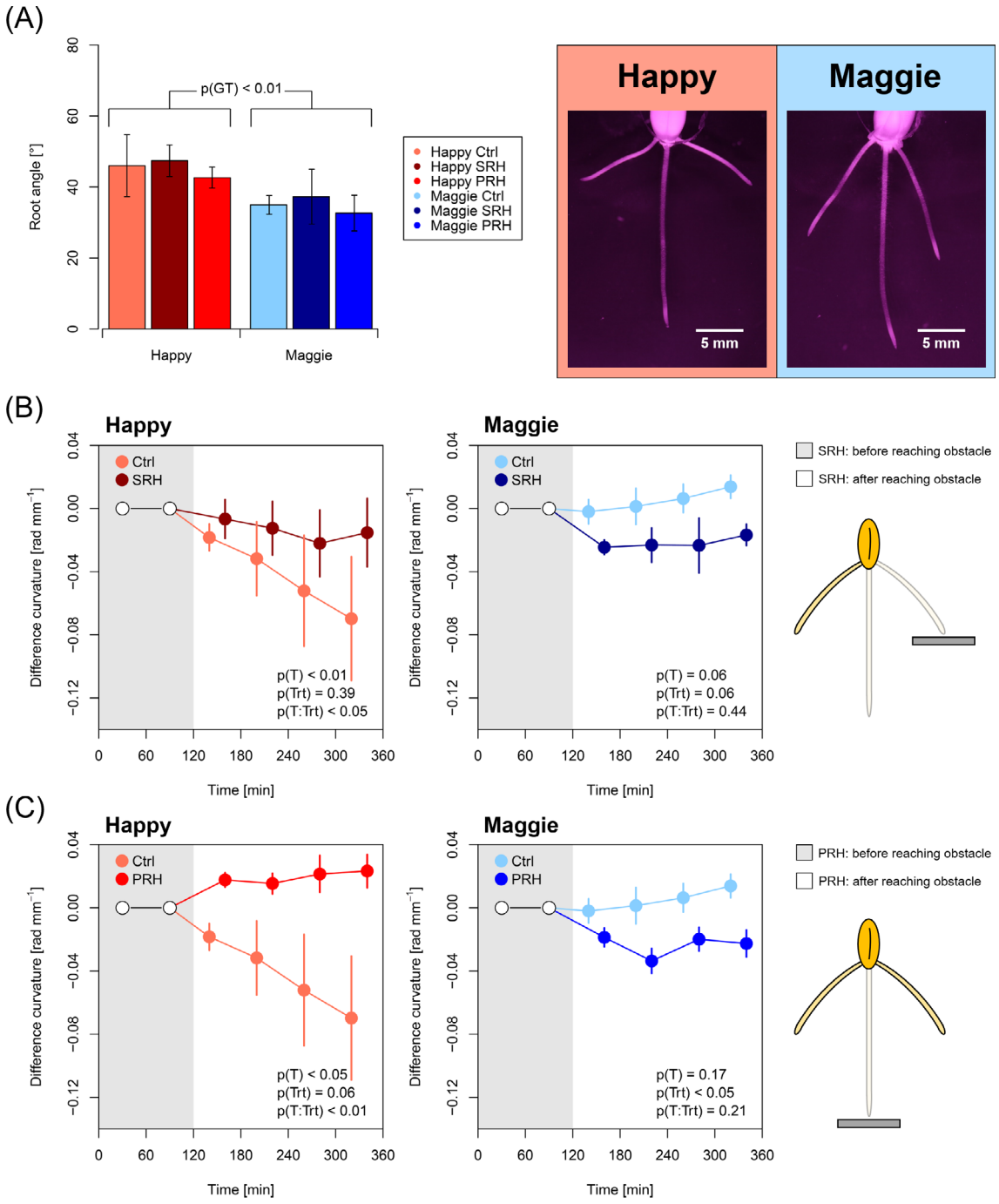

FIGURE 6 Growth direction of unconstrained seminal roots of Happy and Maggie grown without mechanical obstacles (Ctrl) or exposed to horizontal obstacles constraining vertical growth of one seminal root (SRH) or the primary root (PRH). (A) Seminal root angle to the vertical at the beginning of the 6 h measurement period. (B) and (C) Temporal changes in the growth direction of unconstrained seminal roots assessed as the change in curvature of the root growth zone after the first two hours of measurements (Equation 1). Positive and negative differences in curvature indicate shallower and steeper root growth, respectively. Roots of seedlings exposed to obstacles, i.e. SRH and PRH, reached obstacles at Time = 120 min. Error bars denote standard error and *p*-values were derived from (A) analysis of variance models and (B) and (C) linear-mixed models that included the sample effect as a random factor to account for repeated measurements (n = 4).

We showed previously that the root elongation rate is less affected by increasing soil density in Maggie than in Happy (Colombi et al., 2019), corroborating that these two genotypes exhibit contrasting response patterns to soil physical stress. Besides mechanical conditions, dense soil patches and stones influence local soil hydrological and gas transport properties (Naseri et al., 2019; Ebrahimi & Or, 2016), which can have pivotal impacts on root growth and development (Pandey et al., 2021; Gupta et al., 2020). Hence, experiments in soil are needed to gain further insights into the effects of mechanical obstacles on soil exploration. Recent studies identified hormonal

13993054, 2023, 6, Downloaded from https://onlinelibrary.wiley.com/doi/10.1111/ppl.14094 by Inrae - Dipso, Wiley Online Library on [04/04/2024]. See the Terms and Conditions (https://onlinelibrary.wiley.com/terms-and-conditions) on Wiley Online Library for rules of use; OA articles are governed by the applicable Creative Commons License

TABLE 2 Summary statistics on the effects of time (T), treatment (Trt), genotype (GT), and their interactions on the change in growth direction of unconstrained seminal roots. The change in growth direction was quantified as the difference in curvature of the root growth zone during the first two hours, i.e. before the obstacle was reached, and every following hour (Equation 1). *p*-values were derived from linear-mixed models that included the sample effect as a random factor to account for repeated measurements (n = 4)

Trait	Difference in curvature [rad mm^{-1}]
p(T)	0.19
p(Trt)	0.43
p(GT)	0.93
p(T:Trt)	0.09
p(T:GT)	< 0.01
p(Trt:GT)	< 0.05
p(T:Trt:GT)	< 0.01

signalling pathways and underlying genes involved in root phenotypic responses to local differences in water availability (Mehra et al., 2022; Orosa-Puente et al., 2018; Dietrich et al., 2017), highlighting the need to combine molecular and physiological data. Thus, simultaneous quantification of molecular and physiological processes will be crucial to identifying molecular mechanisms and underlying genes that regulate systemic responses to mechanical obstacles in soil.

Avoidance and tolerance are different strategies that contribute to the resistance of plants to environmental stress (Bailey-Serres et al., 2012; Li et al., 2021). The responses to mechanical obstacles observed here suggest that strategies to cope with obstacles in the soil differ between genotypes of the same species. Steeper seminal roots and relatively fast primary root elongation in Maggie suggest stress tolerance, while prioritisation of shallow over deep root growth in combination with more pronounced helical root movement in Happy indicates stress avoidance. Since the current study was conducted with commercially available wheat varieties, we suggest that these different strategies are (presumably unintended) results of plant breeding. Both strategies will likely come with trade-offs that can adversely affect overall plant growth and crop productivity. Increased topsoil exploration (Saengwilai et al., 2014; Gao & Lynch, 2016) and helical root movement (Taylor et al., 2021) reduce the access to subsoil resources, while steep root growth limits the acquisition of nutrients abundant in the topsoil (Sun et al., 2018; Liu et al., 2022b). We, therefore, propose that different strategies to cope with mechanical obstacles may have major impacts on the soil layers in which plants forage for water and nutrients and thus the exploration of heterogeneous soil environments.

5 | CONCLUSIONS

In the current study, we quantified *in vivo* root responses of wheat to mechanical obstacles at high spatiotemporal resolution using time-lapse imaging in conjunction with automated image processing. We showed that constraining vertical growth of a single axial root can affect the elongation rate, helical movement, and the growth direction of unconstrained axial roots of the same plant within a few hours. Hence, we provide evidence for near-immediate systemic responses of roots to mechanical obstacles. Moreover, we demonstrate that different genotypes of the same species can show distinctly different response patterns to localised root impedance, which can be linked to different strategies to cope with mechanical obstacles. Stress avoidance was characterised by shallower root growth and more pronounced helical root movement in response to localised root impedance, while steeper root growth and relatively fast root elongation indicated stress tolerance. We conclude that systemic responses to localised root impedance and different strategies to cope with mechanical obstacles likely play a pivotal role in plant growth under heterogeneous edaphic conditions, which define most soil environments.

AUTHOR CONTRIBUTIONS

TC, VL and MBBT conceived the study; TC, LE, EK and MBBT developed experimental set up and image analysis pipelines; TC and LE conducted experiments; TC analysed the data and wrote the manuscript with input from all co-authors.

ACKNOWLEDGEMENTS

We thank Daniel Iseskog and Mina Spånberg (Department of Soil and Environment, SLU, Uppsala) for help with the experimental set up and Pernilla Vallenback (Lantmännen Lantbruk, Svalöv) for providing the seeds. This study received funding from the Swedish Research Council for Sustainable Development (Formas; grant number: 2019-01189 to TC) and the Lantmännen Research Foundation (grant number: 2019H005 to TC), which is greatly acknowledged.

DATA AVAILABILITY STATEMENT

The data supporting the findings of this study are available from the corresponding author upon reasonable request.

ORCID

Tino Colombi https://orcid.org/0000-0001-8493-4430

REFERENCES

Atkinson, J.A., Hawkesford, M.J., Whalley, W.R., Zhou, H. & Mooney, S.J. (2020) Soil strength influences wheat root interactions with soil macropores. *Plant Cell and Environment*. 43 (1), 235–245. https://doi.org/10.1111/pce.13659.

Bailey-Serres, J., Lee, S.C. & Brinton, E. (2012) Waterproofing Crops: Effective Flooding Survival Strategies. *Plant Physiology*. 160 (4), 1698–1709. https://doi.org/10.1104/pp.112.208173.

Banfield, C.C., Dippold, M.A., Pausch, J., Hoang, D.T.T.T. & Kuzyakov, Y. (2017) Biopore history determines the microbial community composition in subsoil hotspots. *Biology and Fertility of Soils*. 53 (5), 573–588. https://doi.org/10.1007/s00374-017-1201-5.

Bastien, R., Legland, D., Martin, M., Fregosi, L., Peaucelle, A., Douady, S., Moulia, B. & Höfte, H. (2016) KymoRod: a method for automated kinematic analysis of rod-shaped plant organs. *Plant Journal*. 88 (3), 468–475. https://doi.org/10.1111/tpj.13255.

Basu, P., Pal, A., Lynch, J.P. & Brown, K.M. (2007) A Novel Image-Analysis Technique for Kinematic Study of Growth and Curvature. *Plant Physiology*. 145 (2), 305–316. https://doi.org/10.1104/pp.107.103226.

13993054, 2023, 6, Downloaded from https://onlinelibrary.wiley.com/doi/10.1111/ppl.14094 by Inrae - Dipso, Wiley Online Library on [04/04/2024]. See the Terms and Conditions (https://onlinelibrary.wiley.com/terms-and-conditions) on Wiley Online Library for rules of use; OA articles are governed by the applicable Creative Commons License

Bengough, A.G., McKenzie, B.M., Hallett, P.D. & Valentine, T.A. (2011) Root elongation, water stress, and mechanical impedance: a review of limiting stresses and beneficial root tip traits. *Journal of experimental botany*. 62 (1), 59–68. https://doi.org/10.1093/jxb/erq350.

Bingham, I.J. & Bengough, A.G. (2003) Morphological plasticity of wheat and barley roots in response to spatial variation in soil strength. *Plant and Soil*. 250, 273–282.

Bizet, F., Bengough, A.G., Hummel, I., Bogeat-Triboulot, M.-B. & Dupuy, L.X. (2016) 3D deformation field in growing plant roots reveals both mechanical and biological responses to axial mechanical forces. *Journal of Experimental Botany*. 67 (19), 5605–5614. https://doi.org/10.1093/jxb/erw320.

Bizet, F., Hummel, I. & Bogeat-Triboulot, M.B. (2015) Length and activity of the root apical meristem revealed in vivo by infrared imaging. *Journal of Experimental Botany*. 66 (5), 1387–1395. https://doi.org/10.1093/jxb/eru488.

Borer, B., Tecon, R. & Or, D. (2018) Spatial organization of bacterial populations in response to oxygen and carbon counter-gradients in pore networks. *Nature Communications*. 9 (1). https://doi.org/10.1038/s41467-018-03187-y.

Colombi, T., Herrmann, A.M., Vallenback, P. & Keller, T. (2019) Cortical Cell Diameter Is Key To Energy Costs of Root Growth in Wheat. *Plant Physiology*. 180 (4), 2049–2060. https://doi.org/10.1104/pp.19.00262.

Colombi, T., Torres, L.C., Walter, A. & Keller, T. (2018) Feedbacks between soil penetration resistance, root architecture and water uptake limit water accessibility and crop growth – A vicious circle. *Science of The Total Environment*. 626, 1026–1035. https://doi.org/10.1016/j.scitotenv.2018.01.129.

Croser, C., Bengough, A.G. & Pritchard, J. (1999) The effect of mechanical impedance on root growth in pea (Pisum sativum). I. Rates of cell flux, mitosis, and strain during recovery. *Physiologia Plantarum*. 107 (3), 277–286. https://doi.org/10.1034/j.1399-3054.1999.100304.x.

Dexter, A.R. (1986) Model experiments on the behaviour of roots at the interface between a tilled seed-bed and a compacted sub-soil III. Entry of pea and wheat roots into cylindrical biopores. *Plant and Soil*. 95, 149–161.

Dietrich, D., Pang, L., Kobayashi, A., Fozard, J.A., Boudolf, V., et al. (2017) Root hydrotropism is controlled via a cortex-specific growth mechanism. *Nature Plants*. 3 (6), 17057. https://doi.org/10.1038/nplants.2017.57.

Ebrahimi, A. & Or, D. (2016) Microbial community dynamics in soil aggregates shape biogeochemical gas fluxes from soil profiles - upscaling an aggregate biophysical model. *Global Change Biology*. 22 (9), 3141–3156. https://doi.org/10.1111/gcb.13345.

Gao, Y. & Lynch, J.P. (2016) Reduced crown root number improves water acquisition under water deficit stress in maize (Zea mays L.). *Journal of Experimental Botany*. 67 (15), 4545–4557. https://doi.org/10.1093/jxb/erw243.

Gupta, A., Rico-Medina, A. & Caño-Delgado, A.I. (2020) The physiology of plant responses to drought. *Science*. 368 (6488), 266–269. https://doi.org/10.1126/science.aaz7614.

Hinsinger, P., Bengough, A.G., Vetterlein, D. & Young, I.M. (2009) Rhizosphere: biophysics, biogeochemistry and ecological relevance. *Plant and Soil*. 321 (1–2), 117–152. https://doi.org/10.1007/s11104-008-9885-9.

in 't Zandt, D., Le Marié, C., Kirchgessner, N., Visser, E.J.W. & Hund, A. (2015) High-resolution quantification of root dynamics in split-nutrient rhizoslides reveals rapid and strong proliferation of maize roots in response to local high nitrogen. *Journal of Experimental Botany*. 66 (18), 5507–5517. https://doi.org/10.1093/jxb/erv307.

Jin, K., Shen, J., Ashton, R.W., Dodd, I.C., Parry, M.A.J. & Whalley, W.R. (2013) How do roots elongate in a structured soil? *Journal of Experimental Botany*. 64 (15), 4761–4777. https://doi.org/10.1093/jxb/ert286.

Jin, K., White, P.J., Whalley, W.R., Shen, J. & Shi, L. (2017) Shaping an Optimal Soil by Root–Soil Interaction. *Trends in Plant Science*. 22 (10), 823–829. https://doi.org/10.1016/j.tplants.2017.07.008.

Katuwal, K.B., Schwartz, B. & Jespersen, D. (2020) Desiccation avoidance and drought tolerance strategies in bermudagrasses. *Environmental and Experimental Botany*. 171, 103947. https://doi.org/10.1016/j.envexpbot.2019.103947.

Kautz, T., Amelung, W., Ewert, F., Gaiser, T., Horn, R., et al. (2013) Nutrient acquisition from arable subsoils in temperate climates: A review. *Soil Biology & Biochemistry*. 57, 1003–1022.

Keiluweit, M., Wanzek, T., Kleber, M., Nico, P. & Fendorf, S. (2017) Anaerobic microsites have an unaccounted role in soil carbon stabilization. *Nature Communications*. 8 (1), 1–8. https://doi.org/10.1038/s41467-017-01406-6.

Kolb, E., Legué, V. & Bogeat-Triboulot, M.-B. (2017) Physical root–soil interactions. *Physical Biology*. 14 (6), 065004. https://doi.org/10.1088/1478-3975/aa90dd.

Li, P., Ma, B., Palta, J.A., Ding, T., Cheng, Z., Lv, G. & Xiong, Y. (2021) Wheat breeding highlights drought tolerance while ignores the advantages of drought avoidance: A meta-analysis. *European Journal of Agronomy*. 122, 126196. https://doi.org/10.1016/j.eja.2020.126196.

Liu, H., Colombi, T., Jäck, O., Keller, T. & Weih, M. (2022a) Effects of soil compaction on grain yield of wheat depend on weather conditions. *Science of The Total Environment*. 807, 150763. https://doi.org/10.1016/j.scitotenv.2021.150763.

Liu, H., Colombi, T., Jäck, O., Westerbergh, A. & Weih, M. (2022b) Linking wheat nitrogen use to root traits: Shallow and thin embryonic roots enhance uptake but reduce conversion efficiency of nitrogen. *Field Crops Research*. 285, 108603. https://doi.org/10.1016/j.fcr.2022.108603.

Loshchilov, I., Del Dottore, E., Mazzolai, B. & Floreano, D. (2021) Conditions for the emergence of circumnutations in plant roots. *PLoS ONE*. 16 (5), 1–22. https://doi.org/10.1371/journal.pone.0252202.

Lynch, J.P. & Wojciechowski, T. (2015) Opportunities and challenges in the subsoil: pathways to deeper rooted crops. *Journal of Experimental Botany*. 66 (8), 2199–2210. https://doi.org/10.1093/jxb/eru508.

Martínez, I., Chervet, A., Weisskopf, P., Sturny, W.G., Etana, A., Stettler, M., Forkman, J. & Keller, T. (2016) Two decades of no-till in the Oberacker long-term fi eld experiment: Part I. Crop yield, soil organic carbon and nutrient distribution in the soil profile. *Soil & Tillage Research*. 163, 141–151. https://doi.org/10.1016/j.still.2016.05.021.

Martins, A.D., O'Callaghan, F., Bengough, A.G., Loades, K.W., Pasqual, M., Kolb, E. & Dupuy, L.X. (2020) The helical motions of roots are linked to avoidance of particle forces in soil. *New Phytologist*. 225 (6), 2356–2367. https://doi.org/10.1111/nph.16312.

Mehra, P., Pandey, B.K., Melebari, D., Banda, J., Leftley, N., et al. (2022) Hydraulic flux–responsive hormone redistribution determines root branching. *Science*. 378 (6621), 762–768. https://doi.org/10.1126/science.add3771.

Migliaccio, F., Tassone, P. & Fortunati, A. (2013) Circumnutation as an autonomous root movement in plants. *American Journal of Botany*. 100 (1), 4–13. https://doi.org/10.3732/ajb.1200314.

Naseri, M., Iden, S.C., Richter, N. & Durner, W. (2019) Influence of Stone Content on Soil Hydraulic Properties: Experimental Investigation and Test of Existing Model Concepts. *Vadose Zone Journal*. 18 (1), 1–10. https://doi.org/10.2136/vzj2018.08.0163.

Nunan, N., Schmidt, H. & Raynaud, X. (2020) The ecology of heterogeneity: Soil bacterial communities and C dynamics. *Philosophical Transactions of the Royal Society B: Biological Sciences*. 375 (1798). https://doi.org/10.1098/rstb.2019.0249.

Orosa-Puente, B., Leftley, N., von Wangenheim, D., Banda, J., Srivastava, A.K., et al. (2018) Root branching toward water involves posttranslational modification of transcription factor ARF7. *Science*. 362 (6421), 1407–1410. https://doi.org/10.1126/science.aau3956.

13993054, 2023, 6, Downloaded from https://onlinelibrary.wiley.com/doi/10.1111/ppl.14094 by Inrae - Dipso, Wiley Online Library on [04/04/2024]. See the Terms and Conditions (https://onlinelibrary.wiley.com/terms-and-conditions) on Wiley Online Library for rules of use; OA articles are governed by the applicable Creative Commons License

Pandey, B.K., Huang, G., Bhosale, R., Hartman, S., Sturrock, C.J., Jose, L., Martin, O.C., Karady, M., Voesenek, L.A.C.J., Ljung, K., Lynch, J.P., Brown, K.M., Whalley, W.R., Mooney, S.J., Zhang, D. & Bennett, M.J. (2021) Plant roots sense soil compaction through restricted ethylene diffusion. *Science*. 371 (6526), 276–280. https://doi.org/10.1126/science.abf3013.

Pedersen, O., Sauter, M., Colmer, T.D. & Nakazono, M. (2021) Regulation of root adaptive anatomical and morphological traits during low soil oxygen. *New Phytologist*. 229 (1), 42–49. https://doi.org/10.1111/nph.16375.

Pfeifer, J., Faget, M., Walter, A., Blossfeld, S., Fiorani, F., Schurr, U. & Nagel, K. a. (2014) Spring barley shows dynamic compensatory root and shoot growth responses when exposed to localised soil compaction and fertilisation. *Functional Plant Biology*. 41 (6), 581–597. https://doi.org/10.1071/FP13224.

Pinheiro, J., Bates, D., DebRoy, S. & Sarkar, J. (2013) *nlme: Linear and Nonlinear Mixed Effects Models*.

Quiros, M., Bogeat-Triboulot, M.-B., Couturier, E. & Kolb, E. (2022) Plant root growth against a mechanical obstacle: the early growth response of a maize root facing an axial resistance is consistent with the Lockhart model. *Journal of The Royal Society Interface*. 19 (193). https://doi.org/10.1098/rsif.2022.0266.

R Core Team (2020) *R: A Language and Environment for Statistical Computing*. http://www.r-project.org.

Rabot, E., Wiesmeier, M., Schlüter, S. & Vogel, H.J. (2018) Soil structure as an indicator of soil functions: A review. *Geoderma*. 314, 122–137. https://doi.org/10.1016/j.geoderma.2017.11.009.

Roué, J., Chauvet, H., Brunel-Michac, N., Bizet, F., Moulia, B., Badel, E. & Legué, V. (2020) Root cap size and shape influence responses to the physical strength of the growth medium in Arabidopsis thaliana primary roots G. Ingram (ed.). *Journal of Experimental Botany*. 71 (1), 126–137. https://doi.org/10.1093/jxb/erz418.

Ruts, T., Matsubara, S. & Walter, A. (2013) Synchronous high-resolution phenotyping of leaf and root growth in Nicotiana tabacum over 24-h periods with GROWMAP-plant. *Plant Methods*. 9 (1), 1–8. https://doi.org/10.1186/1746-4811-9-2.

Ruts, T., Matsubara, S., Wiese-Klinkenberg, A. & Walter, A. (2012) Diel patterns of leaf and root growth: Endogenous rhythmicity or environmental response? *Journal of Experimental Botany*. 63 (9), 3339–3351. https://doi.org/10.1093/jxb/err334.

Saengwilai, P., Tian, X. & Lynch, J.P. (2014) Low Crown Root Number Enhances Nitrogen Acquisition from Low-Nitrogen Soils in Maize. *Plant Physiology*. 166, 581–589.

Schlüter, S., Eickhorst, T. & Mueller, C.W. (2019) Correlative Imaging Reveals Holistic View of Soil Microenvironments. *Environmental Science and Technology*. 53 (2), 829–837. https://doi.org/10.1021/acs.est.8b05245.

Semchenko, M., Zobel, K., Heinemeyer, A. & Hutchings, M.J. (2008) Foraging for space and avoidance of physical obstructions by plant roots: A comparative study of grasses from contrasting habitats. *New Phytologist*. 179, 1162–1170. https://doi.org/10.1111/j.1469-8137.2008.02543.x.

Sjulgård, H., Iseskog, D., Kirchgessner, N., Bengough, A.G., Keller, T. & Colombi, T. (2021) Reversible and irreversible root phenotypic plasticity under fluctuating soil physical conditions. *Environmental and Experimental Botany*. 188, 104494. https://doi.org/10.1016/j.envexpbot.2021.104494.

Songsri, P., Jogloy, S., Vorasoot, N., Akkasaeng, C., Patanothai, A. & Holbrook, C.C. (2008) Root Distribution of Drought-Resistant Peanut Genotypes in Response to Drought. *Journal of Agronomy and Crop Science*. 194 (2), 92–103. https://doi.org/10.1111/j.1439-037X.2008.00296.x.

Sun, B., Gao, Y. & Lynch, J.P. (2018) Large Crown Root Number Improves Topsoil Foraging and Phosphorus Acquisition. *Plant Physiology*. 177 (1), 90–104. https://doi.org/10.1104/pp.18.00234.

Taylor, I., Lehner, K., McCaskey, E., Nirmal, N., Ozkan-Aydin, Y., Murray-Cooper, M., Jain, R., Hawkes, E.W., Ronald, P.C., Goldman, D.I. & Benfey, P.N. (2021) Mechanism and function of root circumnutation. *Proceedings of the National Academy of Sciences of the United States of America*. 118 (8), 1–10. https://doi.org/10.1073/pnas.2018940118.

Thomson, C.J., Colmer, T.D., Watkin, E.L.J. & Greenway, H. (1992) Tolerance of wheat (Triticum aestivum cvs. Gamenya and Kite) and triticale (Triticosecale cv. Muir) to waterlogging. *New Phytologist*. 120 (3), 335–344.

Tötzke, C., Kardjilov, N., Manke, I. & Oswald, S.E. (2017) Capturing 3D Water Flow in Rooted Soil by Ultra-fast Neutron Tomography. *Scientific Reports*. 7 (1), 1–9. https://doi.org/10.1038/s41598-017-06046-w.

Tracy, S.R., Black, C.R., Roberts, J.A., Sturrock, C., Mairhofer, S., Craigon, J. & Mooney, S.J. (2012) Quantifying the impact of soil compaction on root system architecture in tomato (Solanum lycopersicum) by X-ray micro-computed tomography. *Annals of botany*. 110 (2), 511–519. https://doi.org/10.1093/aob/mcs031.

Vogel, H.J., Bartke, S., Daedlow, K., Helming, K., Kögel-Knabner, I., Lang, B., Rabot, E., Russell, D., Stößel, B., Weller, U., Wiesmeier, M. & Wollschläger, U. (2018) A systemic approach for modeling soil functions. *SOIL*. 4 (1), 83–92. https://doi.org/10.5194/soil-4-83-2018.

Walter, A., Liebisch, F. & Hund, A. (2015) Plant phenotyping: from bean weighing to image analysis. *Plant methods*. 11 (1), 14. https://doi.org/10.1186/s13007-015-0056-8.

Walter, A., Silk, W.K. & Schurr, U. (2009) Environmental effects on spatial and temporal patterns of leaf and root growth. *Annual review of plant biology*. 60, 279–304. https://doi.org/10.1146/annurev.arplant.59.032607.092819.

Wang, X., Whalley, W.R., Miller, A.J., White, P.J., Zhang, F. & Shen, J. (2020) Sustainable Cropping Requires Adaptation to a Heterogeneous Rhizosphere. *Trends in Plant Science*. 25 (12), 1194–1202. https://doi.org/10.1016/j.tplants.2020.07.006.

York, L.M., Carminati, A., Mooney, S.J., Ritz, K. & Bennett, M.J. (2016) The holistic rhizosphere: Integrating zones, processes, and semantics in the soil influenced by roots. *Journal of Experimental Botany*. 67 (12), 3629–3643. https://doi.org/10.1093/jxb/erw108.

Youssef, C., Bizet, F., Bastien, R., Legland, D., Bogeat-Triboulot, M.B. & Hummel, I. (2018) Quantitative dissection of variations in root growth rate: A matter of cell proliferation or of cell expansion? *Journal of Experimental Botany*. 69 (21), 5157–5168. https://doi.org/10.1093/jxb/ery272.

Zarebanadkouki, M., Kim, Y.X. & Carminati, A. (2013) Where do roots take up water? Neutron radiography of water flow into the roots of transpiring plants growing in soil. *New Phytologist*. 199 (4), 1034–1044. https://doi.org/10.1111/nph.12330.

SUPPORTING INFORMATION

Additional supporting information can be found online in the Supporting Information section at the end of this article.

How to cite this article: Colombi, T., Eitelberg, L., Kolb, E., Legué, V. & Bogeat-Triboulot, M.-B. (2023) Genotypic differences in systemic root responses to mechanical obstacles. *Physiologia Plantarum*, 175(6), e14094. Available from: https://doi.org/10.1111/ppl.14094

13993054, 2023, 6, Downloaded from https://onlinelibrary.wiley.com/doi/10.1111/ppl.14094 by Inrae - Dipso, Wiley Online Library on [04/04/2024]. See the Terms and Conditions (https://onlinelibrary.wiley.com/terms-and-conditions) on Wiley Online Library for rules of use; OA articles are governed by the applicable Creative Commons License